Tribology and Materials
Vol. x, No. x, 202x, pp. xx-xx

ISSN 2812-9717
https://doi.org/10.46793/tribomat.2026.018

Thermal performance enhancement in additively manufactured PLA heat sinks through electroplating surface treatment

Harto TANUJAYA *, Kelvin Ferdinand T, Nabil ADITYA

Universitas Tarumanagara, Jakarta, Indonesia
*Corresponding author: hartotan@ft.untar.ac.id

Keywords

heat sink
fin efficiency
electroplating
copper coating
nickel-copper coating
effectiveness

History

Received: 27-07-2026
Revised: 05-10-2026
Accepted: 22-10-2026

Abstract

Additive manufacturing technologies have emerged as a promising alternative manufacturing approach for heat sinks because they accommodate complex finned geometries with shorter fabrication times than conventional machining. A prototype was designed using polylactic acid (PLA), chosen for its low cost, ease of fabrication, biodegradability and direct compatibility with desktop 3D printing. The thermal effectiveness of heat sinks produced by applying copper and copper-nickel coatings through electroplating was analysed through analytical and experimental fin efficiency characterisation. Six samples were tested: three copper-plated heat sinks at deposition currents of 0.75, 1 and 2 A, and three copper-nickel sandwich-coated (two-layer coating; first layer copper and second layer nickel) heat sinks at deposition currents of 0.15, 0.5 and 1 A. The copper-plated heat sink at 2 A produced the highest experimental efficiency of 97.96 % and the tightest analytical and experimental agreement, with a gap of 9.5 %. All of the copper (Cu) and copper-nickel (Cu-Ni) samples reached the dimensionless parameter (mL_c) value between 0.076 and 0.892, indicating the efficiency was still good and suitable for common use as a heat sink. The highest experimental efficiency for Cu-Ni samples was 87.43 %, obtained at a Ni deposition current of 0.15 A. The results show that excessively thick Ni plating produces a measurable reduction in heat sink fin effectiveness, but still gives a Cu-Ni heat sink fin effectiveness between 8 and 11.

1. Introduction

Technological progress has advanced very rapidly and the development of high-performance electronic equipment and systems is increasingly in demand, thus requiring efficient thermal management technology. Electronic components within devices, such as processors, power electronics and thermoelectric parts, generate significant heat during operation. If the heat produced is not effectively removed or minimised, excessive temperature may occur, resulting in degraded performance, shortened component life and the possibility of system failure [1]. Therefore, maintaining the operating temperature of electronic components within acceptable limits is an important issue in electronic system design [2].

The thermal performance of a heat sink depends on many factors, including material properties, heat sink geometry, fin configuration and manufacturing method. Common heat sinks are typically made of metals such as aluminium and copper (Cu) due to their high thermal conductivity [3,4]. These materials, in many cases, involve relatively high production and manufacturing costs, machining complexity and are difficult to use in additive manufacturing [5]. Ez-zine et al. [6] also identified the existence of the minimum melting temperature for optimum purity from recycled copper scrap.

Additive manufacturing technologies are one of the alternative manufacturing approaches becoming more attractive. This type of manufacturing is a promising method for producing heat sinks with complex geometries and shorter

This work is licensed under a Creative Commons Attribution-NonCommercial 4.0 International (CC BY-NC 4.0) license

Article in Press

fabrication times for complex heat sink models. Polylactic acid (PLA) is one of the manufacturing polymer materials with low cost, ease of fabrication, biodegradability and compatibility with desktop 3D printing to make a basic design of the complex's model of a heat sink [7]. The model can be coated by electroplating to improve the thermal conductivity of the polymer-based heat sink model [8]. This method is non-disruptive and low-cost. Several studies have investigated the behaviour of heat sinks and thermal enhancement for heat sinks through geometric model optimisation and material modification [9]. The geometric model optimisation is also discussed by Tanujaya and Darmawan [10] regarding its effectiveness. Ludergnani et al. [11] investigated electroplating using 3D-printed parts made of acrylonitrile butadiene styrene. Perera et al. [12] also experimented with a Cu-electroplated polymer heat sink on Nylon 12. Gibbons et al. [13] also researched metal-coated 3D-printed polymer heat sinks using materials other than PLA. However, experimental investigations of the thermal behaviour of PLA heat sinks, manufactured by additive manufacturing and coated by electroplating, are still relatively limited.

The current research aims to investigate the thermal performance of additively manufactured PLA heat sinks coated by electroplating with copper and nickel. Specifically, it aims to understand how electrochemical coating affects temperature distribution, heat transfer rate and efficiency under controlled experimental conditions.

2. Materials and methods

The current research investigates and evaluates changes in the thermal characteristics of electroplated PLA heat sinks. Firstly, the heat sink model and geometry were designed using Fusion 360 CAD software. The shape has a flat base plate with a fixed size and thickness. The heat sink has a 40 × 40 mm base with fins of 20 mm height, 2.5 mm spacing and a thickness that decreases from the base to the tip, with a tip thickness of 0.6 mm and a mean thickness of 1.36 mm over the whole fin. The fins increase the surface area so the heat sink can cool through natural airflow. The number of fins was 11, as shown in Figure 1.

The heat sink models were manufactured using fused deposition modelling (FDM) on a Creality K2 Plus 3D printer with PLA. PLA filament is commercially available, inexpensive, can be printed at a low temperature, is stiff enough and shapes well for short thermal tests. All heat sink samples were printed with constant parameters: a layer thickness of 0.2 mm, a density of 100 %, a printing speed of 250 mm/s, a bed temperature of 60 °C and a nozzle temperature of 220 °C. After that, all of the heat sink samples were cooled for a few minutes on the printer bed to avoid their shrinkage [14]. After the printing process finished, the heat sinks were checked for quality. Visual inspection was used to examine the heat sink samples for defects common to FDM, such as warping or curling at the base/fin tips, stringing/wisps between fins, non-solid surfaces and layer shift, because surface defects will decrease the quality of the electroplated coatings. Dimensional inspection was also performed by measuring fin thickness, fin spacing, fin height and base size using a Mitutoyo 530-104 Vernier caliper with an accuracy of 0.05 mm and comparing them with the CAD model. Conforming heat sink samples were stored for at least 24 hours before they were coated with graphite.

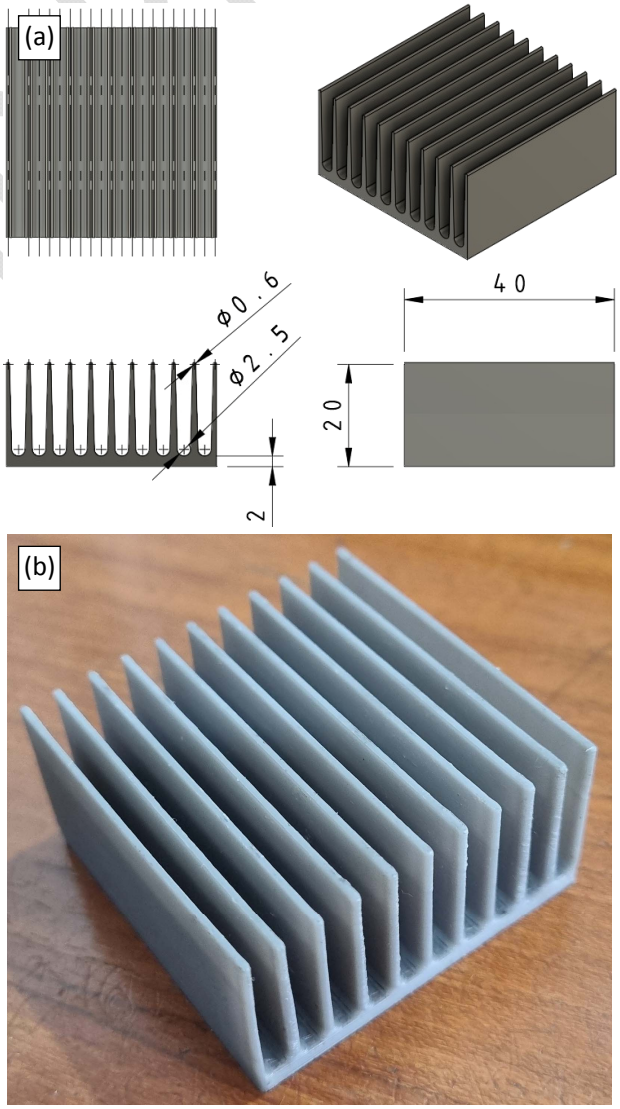


Figure 1. Heat sink model: (a) geometry and (b) 3D-printed PLA

Article in Press

PLA printing does not conduct electricity, so a conductive coating is needed. A conductive surface carries current for Cu electroplating. The conductive layer was made by brushing graphite paint evenly over the whole surface of the printed PLA heat sink. The graphite paint is used as a thin layer that can conduct electrons. Graphit 33 conductive coating spray (Kontakt Chemie, Belgium), with a 20 µm thickness, heat resistance of 250 to 300 °C and surface resistivity of 1000 to 2000 Ω, was used. It converts the insulating PLA surface into one that can conduct current, and it represents the cathode in an electroplating cell [11].

Both copper (Cu) and copper-nickel (Cu-Ni) coatings were deposited by electroplating. Copper was plated for 30 hours on all samples. Nickel was additionally plated for 6 hours on Cu-Ni samples at 0.5 and 1 A, and for 12 hours at 0.15 A. The used two-electrode cell configuration was as follows: the cathode, the working electrode, was the printed PLA heat sink coated with a graphite layer and the anode, the counter electrode, was a copper plate that served as the source of copper ions. Both the cathode and anode were immersed simultaneously in the electrolyte solution, with the electrode spacing held constant at 6 cm for all samples. Acid copper plating as an electrolyte solution for Cu electroplating consists of 250 g $CuSO_4$, 60 ml of H_2SO_4 and 1 l of distilled water. A nickel sulfamate bath is used for Ni electroplating after the Cu electroplating process is finished. This solution is used to produce a thicker, more uniform and lower-stress Ni layer [15,16]. Sulfamate solution consists of nickel sulfamate ($Ni(SO_3NH_2)_2$), nickel chloride ($NiCl_2$) and boric acid (H_3BO_3) and 1 l of distilled water [17]. The current source used was a DC power supply. The current was varied at 0.75, 1 and 2 A to investigate the influence of current on the characteristics of the electroplated copper. Nickel plating was carried out on the heat sink samples that had already been electroplated with copper under the optimum current of 2 A. The current was varied at 0.15, 0.5 and 1A for the electroplating of nickel. All of the samples were visually inspected using a microscope for all fin surfaces, edges and tips after electroplating to detect surface damage or uncoated areas. The thickness of the Cu and Cu-Ni deposits on the heat sink samples, measured using a caliper, was not perfectly uniform over the entire surface. However, the variation was very small, less than 0.1 mm, so the thickness was averaged and the deposits were assumed to be uniform across the surface.

The thermal behaviour of heat sink samples was measured using a UNI-T Uti120S infrared (IR) thermal camera, with a temperature range of –20 to 400 °C. The IR camera has a measurement accuracy of ± 2 °C or ± 2 % and a thermal imaging sensitivity of less than 60 mK. To verify the IR camera measurements, the temperature at the fin base was measured simultaneously with a K-type thermocouple. An emissivity of 0.8 was set, since the Cu and Cu-Ni plated surfaces gave low reflectivity. Figure 2a shows the top-view schematic of the surface temperature measurements performed at predefined points distributed across the heat sink for both Cu and Cu-Ni samples. The 5 points were chosen to be representative of each functional region of the heat sink. The IR thermal camera records a full-field thermal image in which each pixel corresponds to a temperature value, producing a very large number of temperature readings distributed over the entire surface. To analyse and compare the thermal behaviour of the samples in a consistent and repeatable manner, the

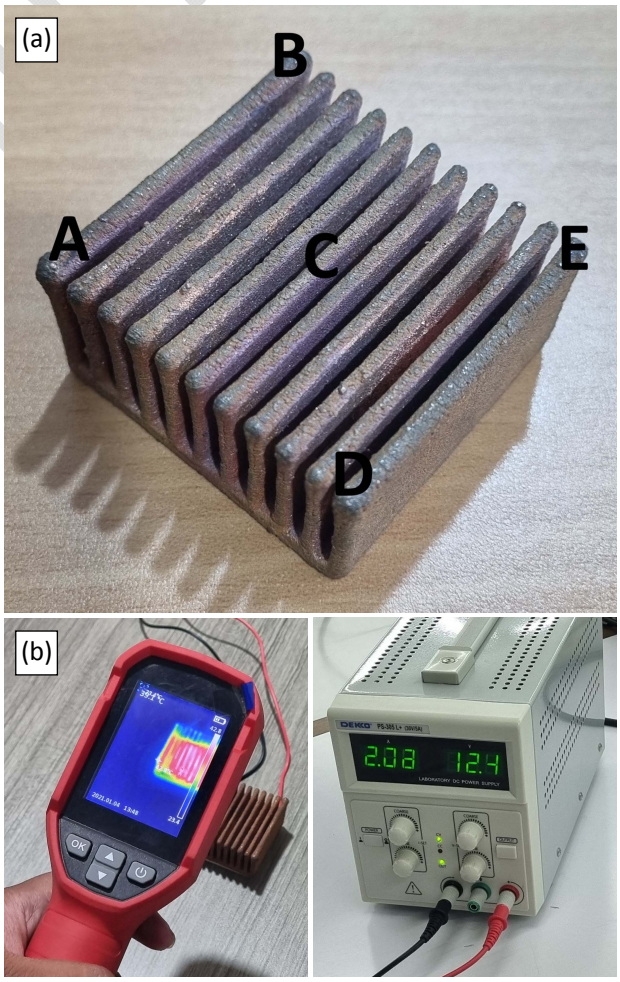


Figure 2. Thermal measurement: (a) surface temperature measurement points and (b) actual test

Article in Press

temperature was therefore extracted at five representative points. Point C is located on the base, points A and B at mid-fin height and points D and E at the fin tip. This approach directs the quantitative evaluation to these specific, well-defined locations rather than to the full temperature distribution. Each experimental condition was measured two times.

Thermal testing was carried out to evaluate the thermal behaviour of electroplated heat sinks. All testing was conducted in similar room conditions, as shown in Figure 2b. This reduced the effect of outside factors such as changes in ambient temperature and airflow around the test rig. A TEC1-12706 Peltier module was used as the heat source. It was chosen because it gives a stable and repeatable heat output. The Peltier module was connected to a DC power supply and set to a voltage of 3.5 V with a current of 0.5 A for all samples. This maintained the ambient temperature at 28 °C for each test.

The heat sink performance is calculated based on a steady-state energy balance. The input electrical power (Q_{max}) as a heat source is calculated from the voltage (V) and current (I) from the DC power supply,

$$Q_{max} = VI, \tag{1}$$

so, at steady state, energy balance can be obtained from actual heat transfer (Q_{act}),

$$Q_{act} = Q_{conv} + Q_{rad} + Q_{loss}. \tag{2}$$

In the present study, the radiative contribution (Q_{rad}) was relatively small but was nevertheless not neglected. It was accounted for through the equivalent radiative heat transfer coefficient, expressed in its linearised form in a formulation analogous to Newton's law of cooling, while heat loss (Q_{loss}) was minimised by good insulation and clean contact.

The convective heat transfer (Q_{conv}) is obtained from the convective heat transfer coefficient (h), the total surface area of the heat sink (A_t), the heat sink surface temperature (T_s) and the ambient temperature (T_∞),

$$Q_{conv} = hA_t(T_s - T_\infty). \tag{3}$$

The surface temperature (T_s) in Equation (3) was obtained by averaging the temperature values recorded between the 2nd and 16th minutes of the test, while the ambient temperature was 28 °C. Furthermore, Q_{act} is equal to Q_{conv}, so the heat flow that occurs can be calculated. The total surface area (A_t) is calculated by summing the base and fins of the heat sink,

$$A_t = NA_f + A_b, \tag{4}$$

where N is the number of fins, A_f is the area of one fin and A_b is the unfinned base surface area of the upper plate, i.e. the portion of the base between the fins that is directly exposed to the cooling fluid.

Calculation of fins requires a corrected fin length (L_c), which is obtained from

$$L_c = L + \frac{t}{2}, \tag{5}$$

where L is the fin length and t is the fin thickness.

The fin profile area (A_p) is calculated from the corrected fin length (L_c) and fin thickness (t),

$$A_p = L_c t. \tag{6}$$

The dimensionless parameter (mL_c) based on the fin parameter (m) and corrected fin length (L_c) is calculated as [18]

$$mL_c = \left(\frac{2h}{kA_p}\right)^{\frac{1}{2}} L_c^{\frac{3}{2}}, \tag{7}$$

where k is the thermal conductivity of the fin material, which influences the performance of the heat sink.

The thermal conductivity values used in the analytical calculation in Equation (7) were taken as k_{PLA} = 0.12 W/mK, k_{Cu} = 385 W/mK and k_{Ni} = 90 W/mK. For the uncoated PLA fin, a single-layer model was used, with the thermal conductivity of PLA. For the coated fins, a multi-layer model was used, with the effective thermal conductivity of the layered fin calculated as a thickness-weighted average. The layer thicknesses were taken from the dimensional measurements. The thermal conductivity value entering the calculation was assigned sequentially for each layer of the Cu and Cu-Ni plated heat sink samples, based on the layer material, its average thickness and the thermal conductivity of the corresponding material.

The analytical efficiency of an individual fin (η_f) is determined by Holman [19],

$$\eta_f = \frac{\tanh(mL_c)}{mL_c}, \tag{8}$$

so the overall analytical efficiency (η_o) of the heat sink is obtained as [20],

$$\eta_o = 1 - \frac{NA_f}{A_t}(1 - \eta_f). \tag{9}$$

Article in Press

The actual (experimental) heat sink efficiency (η_{act}) is defined as the ratio of the actual heat transfer (Q_{act}), which is obtained from experiments, to the maximum possible heat transfer from the input electrical power (Q_{max}), as

$$\eta_{act} = \frac{Q_{act}}{Q_{max}}. \quad (10)$$

The enhancement in heat transfer performance obtained by adding fins to a heat sink, relative to the same heat sink without fins, is expressed by the overall fin effectiveness ($\varepsilon_{fin,\,overall}$), defined as [20],

$$\varepsilon_{fin,overall} = \frac{A_b + \eta_o N A_f}{A_{no\,fin}}, \quad (11)$$

where $A_{no\,fin}$ is the area of the bottom base surface, free of fins.

3. Results and discussion

The electroplated samples were first evaluated by visual inspection. Cu and Ni layers were formed on the surface of all heat sink samples, but the quality of the layers varied for the tested current levels of 0.75, 1, and 2 A for Cu and 0.15, 0.5 and 1 A for Ni, as shown in Figure 3.

Figures 3a, 3b and 3c show the Cu coating electroplated at 2, 1 and 0.75 A. The dimensional measurements in Table 1 confirm that the higher deposition rate at 2 A produced a considerably thicker Cu layer compared with those deposited at 1 and 0.75 A. In this case, the deposited Cu was thick enough at the top corner of the fin tips to partially close the gaps between the tips of adjacent fins, particularly at 1 and 0.75 A, which narrows the airflow passage and reduces the fin effectiveness in releasing heat to the surrounding air. The coating thickness was determined from the change in the outer dimensions of the heat sink measured before and after electroplating. At 0.75 A, the coverage of the surface with the coating was incomplete, i.e. some regions of the heat sink surface were only partly coated. Among the conditions tested, an electroplating current of 2 A, applied for 30 hours, gave the most balanced result and was therefore adopted as the optimal condition for the subsequent stage of Ni electroplating.

Figures 3d, 3e and 3f show the Cu-Ni coating electroplated at 1, 0.5 and 0.15 A. All three samples were fully covered by a Ni layer, i.e. no uncoated patches were noticed on the heat sink surface. The main difference between the

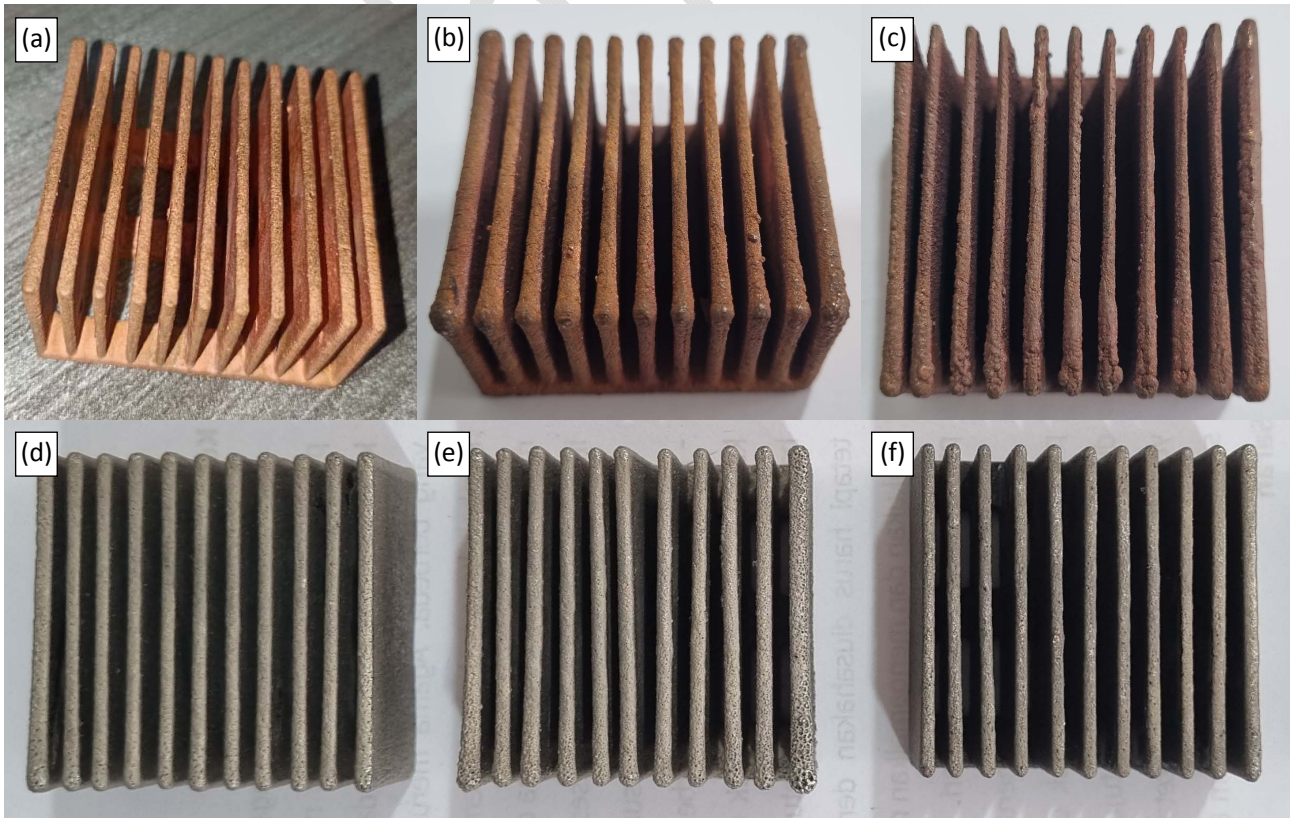


Figure 3. Electroplated heat sink samples: (a) Cu-2A, (b) Cu-1A, (c) Cu-0.75A, (d) Cu-Ni-1A, (e) Cu-Ni-0.5A and (f) Cu-Ni-0.15A

Table 1. Outer dimensions and coating thickness after electroplating

Sample	Length, mm		Width, mm		Height, mm	
	dimension	thickness	dimension	thickness	dimension	thickness
Cu-0.75A	41.16	1.16	40.85	0.85	21.28	1.28
Cu-1A	41.76	1.76	41.55	1.55	21.34	1.34
Cu-2A	42.17	2.17	41.50	1.50	21.45	1.45
Cu-Ni-0.15A	41.50 (Cu) 41.63 (Cu-Ni)	1.50 (Cu) 0.13 (Ni)	40.52 (Cu) 40.60 (Cu-Ni)	0.52 (Cu) 0.08 (Ni)	20.80 (Cu) 20.90 (Cu-Ni)	0.80 (Cu) 0.10 (Ni)
Cu-Ni-0.5A	42.15 (Cu) 42.20 (Cu-Ni)	2.15 (Cu) 0.05 (Ni)	41.10 (Cu) 41.17 (Cu-Ni)	1.10 (Cu) 0.07 (Ni)	21.01 (Cu) 21.08 (Cu-Ni)	1.01 (Cu) 0.07 (Ni)
Cu-Ni-1A	42.06 (Cu) 42.70 (Cu-Ni)	2.06 (Cu) 0.64 (Ni)	40.80 (Cu) 41.13 (Cu-Ni)	0.80 (Cu) 0.33 (Ni)	21.47 (Cu) 21.56 (Cu-Ni)	1.47 (Cu) 0.09 (Ni)

samples was the thickness of the Ni layer, which increased as the electroplating current increased. The surface morphology also differed with the current. The sample electroplated at 0.15 A had the smoothest and most uniform surface. The sample electroplated at 0.75 A showed a slightly rougher surface than 0.15 A. The sample electroplated at 1 A showed the highest surface roughness, with clearly visible macrogeometrical imperfections. This trend is consistent with published studies on nickel electroplating, which report that lower current densities generally produced finer surface textures [15].

The thickness of the deposited layers was measured after electroplating. The outer dimensions (length × width × height) increased as the applied electroplating current increased. As shown in Table 1, the sample electroplated at 0.75 A had the smallest dimensions of 41.16 × 40.85 × 21.28 mm. The sample electroplated at 1 A had larger dimensions in every direction (41.76 × 41.55 × 21.34 mm), and the sample electroplated at 2 A was the largest, with the outer dimensions of 42.17 × 41.50 × 21.45 mm. The Cu-Ni coatings also show a trend of larger outer dimensions as the current increases.

Figure 4 shows the visual distribution of temperature measured with the IR thermal camera. The camera was placed at the same position for every test. The distance, angle and relative position were kept the same. The mean surface temperature and temperature distribution are analysed from these images [21]. These full-field thermal images are retained as a visual overview, while the pointwise values (Fig. 2a) provide the quantitative basis for the fin efficiency and effectiveness calculations.

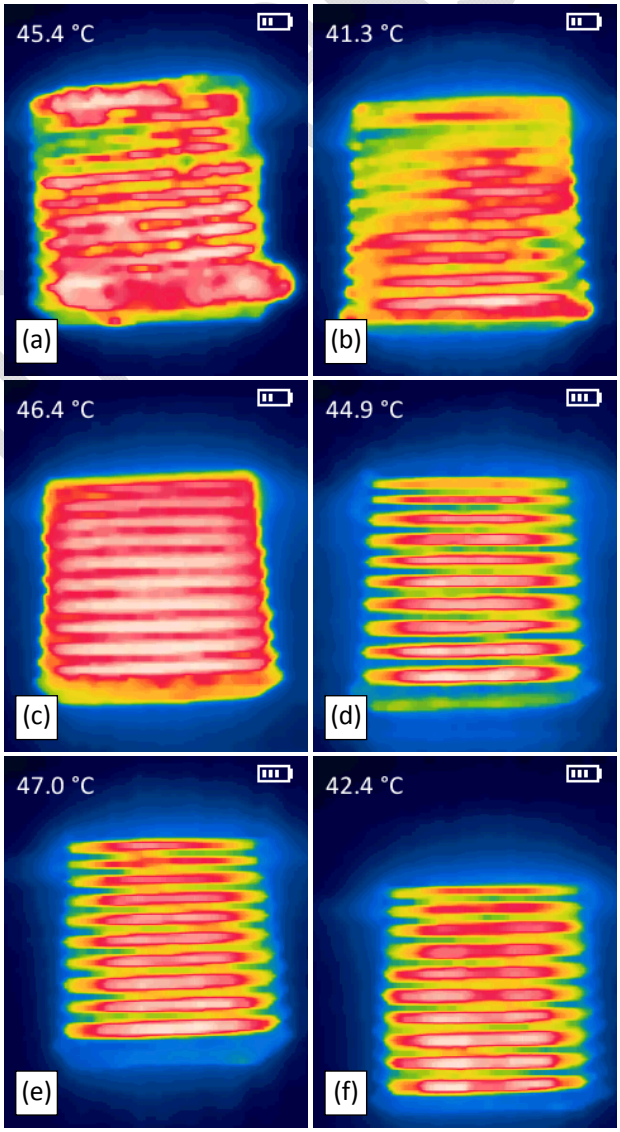


Figure 4. Visual distribution of temperature during the testing of samples: (a) Cu-2A, (b) Cu-1A, (c) Cu-0.75A, (d) Cu-Ni-1A, (e) Cu-Ni-0.5A and (f) Cu-Ni-0.15A

Figures 5a and 5b show the thermal behaviour of the heat sink Cu samples deposited with 0.75, 1 and 2 A current and Cu-Ni samples deposited with

Article in Press

0.15, 0.5 and 1 A current. The mean surface temperature of each Cu electroplated sample was determined as the average of the temperature readings recorded at the five predefined measurement points A-E (Fig. 2a). As shown in the figure, the mean surface temperature increased gradually over the 16 min testing and approached a steady-state value during the last 4 minutes. The Cu-0.75A sample temperature increased from 38.6 °C at 2 min to 43.7 °C at 16 min, with the five measurement points following each other closely and a maximum reading of 43.7 °C recorded at 10, 12 and 16 min, indicating a uniform temperature distribution across the sample but yielding the second-highest temperature of all samples tested. The Cu-1A sample temperature increased from 36.4 to 41.2 °C, which is lower and smoother than the Cu-0.75A sample curve, with a steady-state range of 40 to 41.2 °C reached from 12 min onwards and a similarly tight point-to-point spread. The Cu-2A sample temperature increased from 39.0 to 43.9 °C, making it the warmest of the three Cu electroplated samples, with a noticeably larger point-to-point spread, with a maximum reading of 43.9 °C at 16 min and 43.6 °C at 10 min, confirming that the high current induces a thicker and less uniform deposit that partially closed the inter-fin gaps and reduced the effective cooling area. Overall, the optimum electroplating current is 1 A rather than the highest one tested. Lower current at 0.75 A produces an acceptable but unoptimised deposit, while too-high current at 2 A makes the deposit so thick and uneven that it negatively affects the aesthetic.

The Cu-Ni-1A sample temperature increased from 36.9 to 46.2 °C over the first six readings, followed by a decrease to 44.9 and 38.3 °C at the last two readings. The mean of the eight readings was 41.0 °C, with a peak of 46.2 °C. The temperature increased from 36.9 to 38.3 °C from 2 to 16 min, which means that an increase of only 1.4 °C occurred during the 16 min testing. This suggests that the sample approached a quasi-steady-state value of approximately 38 to 39 °C before being affected by a localised transient at 12 min, which increased the temperature to 46.2 °C. The point-to-point range of 12.9 °C is moderate and consistent with moderately uniform Cu-Ni deposits. The pattern for the Cu-Ni-0.5A sample is broadly similar. It starts at 33.6 °C, increases through 38.8 to 43.0 °C, and decreases to 38.7 and 38.9 °C, then increases again to 46.4 and 47.0 °C. The mean of the eight readings was 40.9 °C, which is almost the same as the Cu-Ni-1A sample. The temperature increased from 33.6 to 40.4 °C with an increase of 6.8 °C, and the maximum temperature of 47.0 °C is the second-highest single reading of the three Cu-Ni samples. The Cu-Ni-0.5A and Cu-Ni-1A samples therefore have nearly identical thermal behaviour. The Cu-Ni-0.15A sample shows the worst thermal behaviour of the three Cu-Ni samples. The mean of the eight readings was 43.6 °C, which is approximately 2.6 to 2.7 °C warmer than the Cu-Ni-0.5A and Cu-Ni-1A samples. The temperature increased from 37.0 to 42.7 °C with an increase of 5.7 °C, which was the highest of all three Cu-Ni samples. The maximum value of 49.4 °C is the highest single value for all three Cu-Ni samples, and the data show the most erratic profile, with two distinct peaks of 45.4 and 48.1 °C, separated by a decrease to 43.4 °C and a third peak at 49.4 °C.

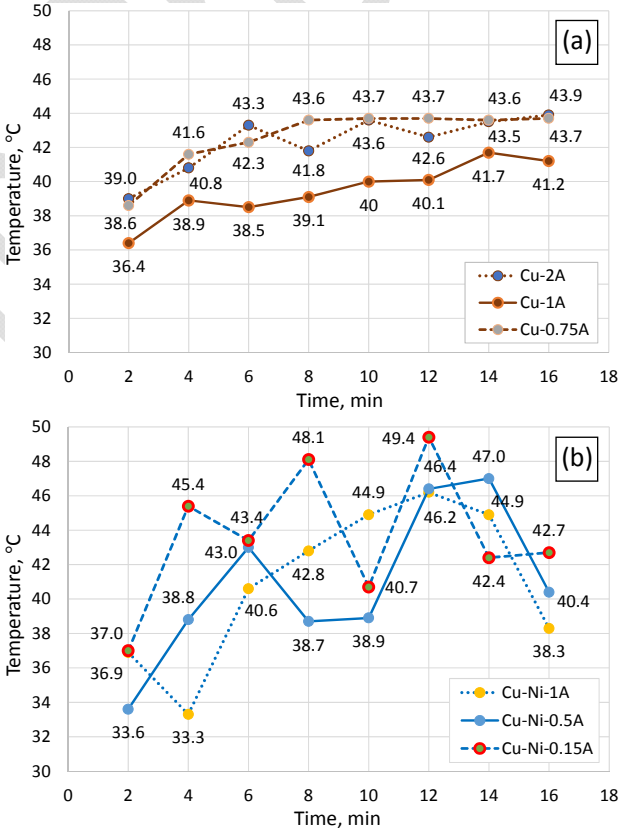


Figure 5. Thermal behaviour of samples: (a) Cu deposits and (b) Cu-Ni deposits

Figure 6 shows the comparison of analytical and experimental efficiency, the average surface temperature, and the dimensionless parameter (mL_c) of the heat sink samples electroplated with different materials and at different currents. The parameter mL_c represents the balance of heat conduction within the fin and heat loss by convection from the fin surface to the surrounding air. It also enables the prediction and assessment

Article in Press

of fin characteristics, which helps in the optimisation of the overall heat sink design, including fin length and thickness, as well as material selection. Figure 6 shows that the Cu-2A sample has the lowest mL_c of 0.076, which is closest to the origin and consistent with its analytical efficiency of 97.96 %. The analytical efficiency of an individual fin obtained from Equation (8) was calculated using the standard expression for a fin of uniform cross-section, while the dimensionless parameter mL_c was obtained using Equation (7). The experimental efficiency was obtained from Equation (10), where the actual heat transfer was determined from the measured experimental data. The other samples have mL_c values between 0.106 and 0.892, which is the regime of most heat sinks and is classified as a high efficiency of approximately 85 to 95 % [22]. Figure 6 also shows that the relationship between parameter mL_c and experimental efficiency is non-monotonic and non-trivial. This means that a high value of mL_c does not automatically imply high experimental heat sink efficiency and vice versa.

The experimental efficiency formulation adopted in the present heat sink research follows the method of Tanujaya and Sukania [23], which expresses performance on a capacity rate basis. In Figure 6, the Cu-2A sample shows a small gap between analytical (97.96 %) and experimental (88.46 %) efficiency of 9.5 %. This indicates that the deposit quality at the 2 A current does not strongly affect the efficiency. The Cu-1A sample shows the largest efficiency gap of 16.75 % among the Cu electroplated samples, with analytical efficiency of 97.23 % and experimental efficiency of 80.48 %. The Cu-0.75A sample has an efficiency gap of 8.73 % between analytical (96.12 %) and experimental (87.39 %) efficiency. This indicates that the sample has a deposit thickness too low to have an effect on the conduction. The Cu-Ni-1A sample shows the largest efficiency gap of 25.36 % among the Cu-Ni electroplated samples, with analytical efficiency of 90.13 % and experimental efficiency of 64.77 %. This indicates that depositing a Ni coating that is too thick will reduce the overall thermal efficiency of the heat sink, as Ni has a lower thermal conductivity than Cu. The Cu-Ni-0.5A sample has an efficiency gap of 14.63 % between analytical (90.12 %) and experimental (75.49 %) efficiency. Ni electroplating with a current of 0.5 A gives a smoother deposit and a smaller gap between analytical and experimental efficiency than with a current of 1 A. Among the Cu-Ni samples, the sample electroplated at a current of 0.15 A showed the closest agreement between the analytical and experimental efficiency, with the smallest efficiency gap of 2.38 % among all the tested samples. Its analytical efficiency was 89.81 % and its experimental efficiency was 87.43 %. This indicates that the current of 0.15 A produces a Ni deposit so thin that the heat sink is effectively behaving more like the underlying Cu coating than a full Cu-Ni coating.

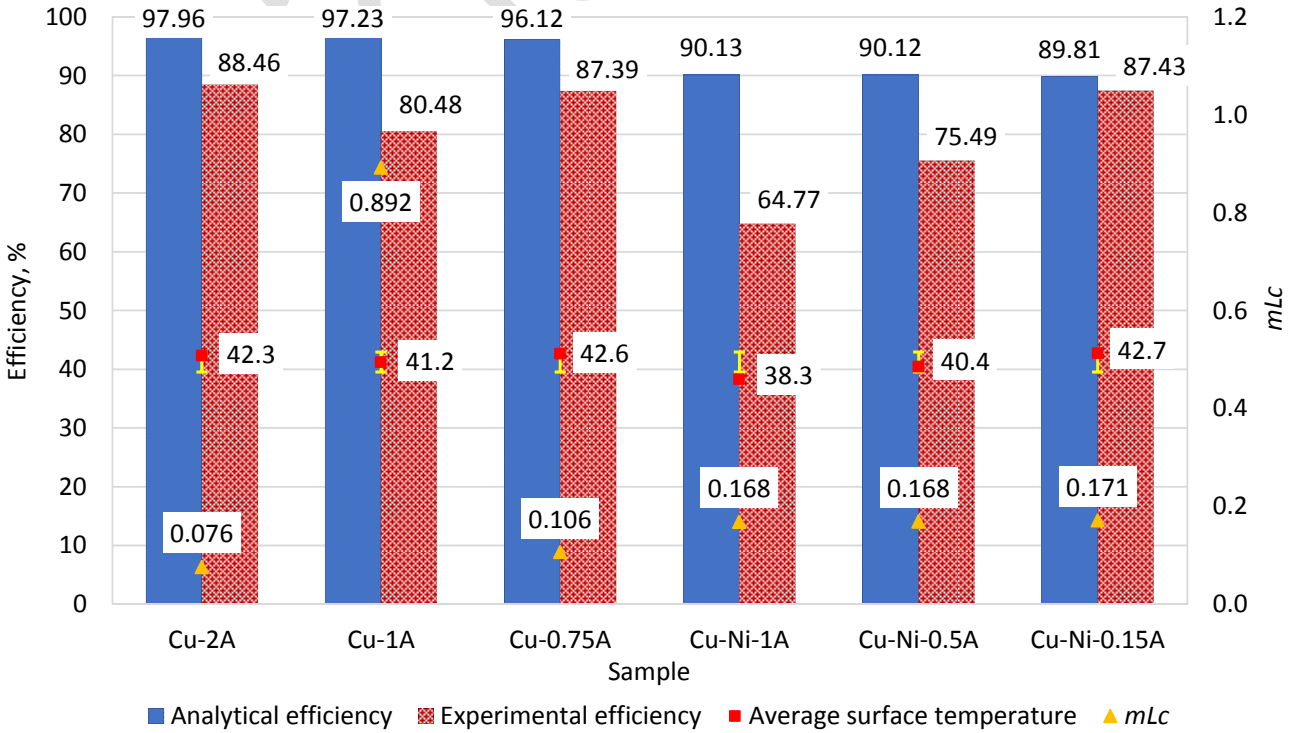


Figure 6. Efficiency, average surface temperature and dimensionless parameter mL_c of the tested heat sink samples

Figure 7 shows the effectiveness of the tested heat sink samples. An assessment of the overall analytical efficiency of an unplated PLA heat sink, using Equation (9), indicates that the efficiency of a 3D-printed heat sink model made of PLA can be enhanced to reach values between 8 and 11.

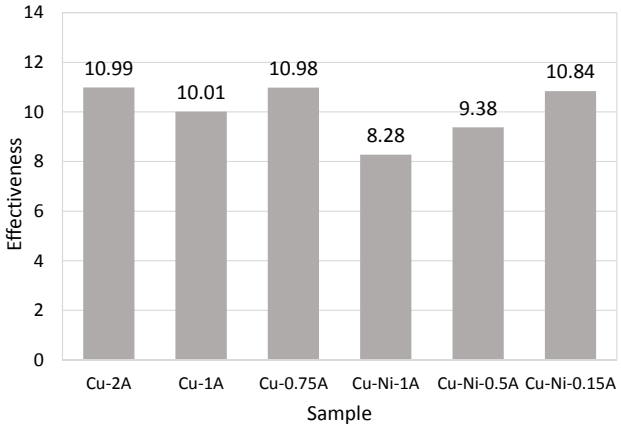


Figure 7. Effectiveness of the tested heat sink samples

4. Conclusion

In the present study, heat sinks manufactured from PLA by fused deposition modelling were successfully electroplated with Cu and Cu-Ni coatings, demonstrating a practical route for improving the heat-dissipation capability of additively manufactured polymer components. The layer deposited through electroplating covered the whole fin surface, including the fin-tip areas, with Cu thickness varying between 0.85 and 2.17 mm and Cu-Ni layers thickness between 0.52 and 2.15 mm (Cu layer) and 0.05 to 0.64 mm (Ni layer). The thermal characterisation performed with an IR thermal camera showed that the electroplated heat sinks provided effective heat-transfer performance. The Cu heat sink samples provided higher efficiencies than the Cu-Ni heat sink samples. For the Cu heat sink samples, the analytical efficiency decreased from 97.96 to 96.12 % and experimental efficiency decreased from 88.46 to 80.48 %, as the deposition current was reduced from 2 to 0.75 A. For the Cu-Ni heat sink samples, the highest analytical efficiency of 90.13 % was obtained at a deposition current of 1 A, and the highest experimental efficiency of 87.43 % was obtained at a deposition current of 0.15 A. Overall, the Cu heat sink samples deposited at a current of 2 A provided the best thermal performance, corresponding to the highest efficiency and effectiveness of 10.99. Analytically, this result indicates that the heat transfer of the 3D-printed heat sink model made from PLA can be enhanced and can achieve an effectiveness between 8 and 11.

Acknowledgement

This study was supported and funded by the Institute of Research and Community Engagement (LPPM), Universitas Tarumanagara, Indonesia. The authors wish to thank all of the participating personnel for their help, support and suggestions.

References

[1] L.T. Yeh, Review of heat transfer technologies in electronic equipment, Journal of Electronic Packaging, Vol. 117, No. 4, 1995, pp. 333-339, DOI: 10.1115/1.2792113

[2] A.R. Dhumal, A.P. Kulkarni, N.H. Ambhore, A comprehensive review on thermal management of electronic devices, Journal of Engineering and Applied Science, Vol. 70, 2023, Paper 140, DOI: 10.1186/s44147-023-00309-2

[3] H. Igarashi, M. Hirota, M. Yoshida, T. Miyashita, Design optimization of fin shape of heat sinks for enhanced cooling performance, in Proceedings of the 2022 International Conference on Electronics Packaging (ICEP 2022), 11-14.05.2022, Sapporo, Japan, pp. 105-106, DOI: 10.23919/ICEP55381.2022.9795403

[4] X.Q. Lim, M.S. Abdul Aziz, C.Y. Khor, J.P. Simanjuntak, Influence of heat sink material and surface coatings on passive cooling thermal performance, Journal of Electronic Materials, Vol. 55, No. 2, 2026, pp. 1522-1536, DOI: 10.1007/s11664-025-12284-w

[5] Y. Cormier, P. Dupuis, B. Jodoin, A. Corbeil, Pyramidal fin arrays performance using streamwise anisotropic materials by cold spray additive manufacturing, Journal of Thermal Spray Technology, Vol. 25, No. 1-2, 2016, pp. 170-182, DOI: 10.1007/s11666-015-0267-6

[6] M. Ez-zine, O. Choukri, S. Taibi, Impact of thermal pretreatment process on recycled copper purity, Tribology and Materials, Vol. 4, No. 3, 2025, pp. 155-164, DOI: 10.46793/tribomat.2025.012

[7] B.M. Nafis, R. Whitt, A.-C. Iradukunda, D. Huitink, Additive manufacturing for enhancing thermal dissipation in heat sink implementation: A review, Heat Transfer Engineering, Vol. 42, No. 12, 2021, pp. 967-984, DOI: 10.1080/01457632.2020.1766246

[8] K. Gautam, D. Gogoi, T.D. Kongnyui, S. Devi, C. Kumar, M. Kumar, A comprehensive review on surface modifications of polymer-based 3D-printed structures: Metal coating prospects and challenges, Polymers for Advanced

Article in Press

Technologies, Vol. 35, No. 4, 2024, Paper e6369, DOI: 10.1002/pat.6369
[9] N. Elmrabet, P. Siegkas, Dimensional considerations on the mechanical properties of 3D printed polymer parts, Polymer Testing, Vol. 90, 2020, Paper 106656, DOI: 10.1016/j.polymertesting.2020.106656
[10] H. Tanujaya, S. Darmawan, Investigation of flow of the disc-and-doughnut baffles and 40% cut segmental baffles, International Journal of Heat and Technology, Vol. 39, No. 5, 2021, pp. 1541-1548, DOI: 10.18280/ijht.390516
[11] T. Ludergnani, G. Fredi, L. Malagutti, A. Balbo, A. Dorigato, F. Mollica, V. Mazzanti, Infill density effects on the mechanical and thermal properties of copper-plated 3D printed parts, Macromolecular Materials and Engineering, Vol. 308, No. 12, 2023, Paper 2300203, DOI: 10.1002/mame.202300203
[12] I.U. Perera, N. Narendran, J.P. Freyssinier, 3D-printed heat sinks for thermal management of LED lighting, Proceedings of SPIE, Vol. 12670, 2023, Paper 1267009, DOI: 10.1117/12.2676953
[13] M.J. Gibbons, C. Feng, S. Chandra, Composite heat sink LED cooling, in Proceedings of The Canadian Society for Mechanical Engineering International Congress 2018, 27-30.05.2018, Toronto, Canada, Paper 213, DOI: 10.25071/10315/35377
[14] J. Zhan, J. Cai, R. Hasani, Effects of testing speed on the tensile and mode I fracture behavior of specimens printed through the fused deposition modeling technique, Scientific Reports, Vol. 14, 2024, Paper 3960, DOI: 10.1038/s41598-024-54780-9
[15] A. Boukhouiete, S. Boumendjel, N.-E.-H. Sobhi, Effect of current density on the microstructure and morphology of the electrodeposited nickel coatings, Turkish Journal of Chemistry, Vol. 45, No. 5, 2021, pp. 1599-1608, DOI: 10.3906/kim-2102-46
[16] T. Müller, S. Scholz, M. Ehrhardt, S. Ruíz Trujillo, M. Cogollo de Cádiz, A. Díaz Lantada, M. Guttmann, Hybridizing 3D printing and electroplating for the controlled forming of metal structures within fused deposition modelled contours, The International Journal of Advanced Manufacturing Technology, Vol. 136, No. 10, 2025, pp. 4369-4381, DOI: 10.1007/s00170-025-15089-7
[17] A. Yli-Pentti, Electroplating and electroless plating, in S. Hashmi, G. Ferreira Batalha, C.J. Van Tyne, B. Yilbas, Comprehensive Materials Processing, Volume 4, Elsevier, Amsterdam, 2014, pp. 277-306, DOI: 10.1016/B978-0-08-096532-1.00413-1
[18] F.P. Incropera, D.P. DeWitt, T.L. Bergman, A.S. Lavine, Fundamentals of Heat and Mass Transfer, John Wiley & Sons, Hoboken, 2007.
[19] J.P. Holman, Heat Transfer, McGraw-Hill, New York, 2010.
[20] Y.A. Çengel, A.J. Ghajar, Heat and Mass Transfer: Fundamentals & Applications, McGraw-Hill Education, New York, 2015.
[21] D. Martínez-Maradiaga, A. Damonte, A. Manzo, J.H.K. Haertel, K. Engelbrecht, Design and testing of topology optimized heat sinks for a tablet, International Journal of Heat and Mass Transfer, Vol. 142, 2019, Paper 118429, DOI: 10.1016/j.ijheatmasstransfer.2019.07.079
[22] J.-C. Han, L. M. Wright, Analytical Heat Transfer, CRC Press, Boca Raton, 2022, DOI: 10.1201/9781003164487
[23] H. Tanujaya, I.W. Sukania, Experimental study of stationary-head/channel cover STHE prototype using ε-NTU method, Experimental Techniques, Vol. 43, No. 6, 2019, pp. 645-655, DOI: 10.1007/s40799-019-00322-2

Article in Press